JACS
JOURNAL OF THE AMERICAN CHEMICAL SOCIETY
Communication
pubs.acs.org/JACS

A Magnetostructural Investigation of an Abrupt Spin Transition for 1-Phenyl-3-trifluoromethyl-1,4-dihydrobenzo[*e*][1,2,4]triazin-4-yl

Christos P. Constantinides,[†] Andrey A. Berezin,[†] Georgia A. Zissimou,[†] Maria Manoli,[†] Gregory M. Leitus,[‡] Michael Bendikov,[‡] Michael R. Probert,[§] Jeremy M. Rawson,[∥] and Panayiotis A. Koutentis*[,†]

[†]Department of Chemistry, University of Cyprus, P.O. Box 20537, 1678 Nicosia, Cyprus
[‡]Department of Organic Chemistry, Weizmann Institute of Science, 76100 Rehovot, Israel
[§]School of Chemistry, Newcastle University, Newcastle upon Tyne NE1 7RU, United Kingdom
[∥]Department of Chemistry & Biochemistry, University of Windsor, 401 Sunset Avenue, Windsor, ON N9B 3P4, Canada

Supporting Information

ABSTRACT: 1-Phenyl-3-trifluoromethyl-1,4-dihydrobenzo[*e*][1,2,4]triazin-4-yl is the first example of a hydrazyl radical that shows a reversible sharp spin transition fully completed within 5(1) K. The nominally first-order transition takes place at ca. 58(2) K and proceeds via subtle changes of intra- and interstack interactions between two similar structural phases. The low-temperature phase (5−60 K) is diamagnetic and has a singlet ground state ($2J_{exp} = -166.8$ cm^{-1}, $g_{solid} = 2.0042$, $\rho = 0.2\%$) stemming from a multicenter two-electron interaction. The high-temperature phase (60−300 K) is paramagnetic as a result of noninteracting $S = {}^1/_2$ spins arising from weakly bound dimers.

The potential of organic persistent radicals to be used as multifunctional materials in electronic devices is becoming attractive and promising.[1] The presence of unpaired electrons provides the opportunity to combine magnetic, optical, and transport properties in a single material. External stimuli such as heat, light, or pressure can be used to tune these unique physical properties, although to date only a few examples have been reported.[2,3] The response to these external stimuli is directly associated with the ability to switch between spin states.

A prerequisite for organic radicals to demonstrate spin transition behavior is a low dimerization enthalpy ($\Delta H_{dim} \approx 0$) and the presence of two similar structural phases related by small atomic displacements, one with an enthalpy-favored low-spin configuration and the other with an entropy-favored high-spin configuration. Many classes of organic radicals have low dimerization enthalpies, but to date the structural reorganization required for a spin transition has mainly been observed in 1,3,2-dithiazolyls.[3,4] Nevertheless, three more examples of spin-transition radicals have been reported (a spirophenalenyl,[5a] a phenoxyl,[5b] and a nitroxide[5c]), indicating that this behavior can exist in other classes of organic radicals with $\Delta H_{dim} \approx 0$.

Hydrazyls have long been known to have low dimerization enthalpies.[6] To date, no spin transition has been observed for any member of this class of radicals. 1,2,4-Benzotriazinyls, a subclass of hydrazyls, have recently attracted attention because of their enhanced air and moisture stability.[7] Although they were first prepared by Blatter in the late 1960s, only sporadic work on this radical class has been reported, in stark contrast to the closely related verdazyl radicals.[8] Within the context of our ongoing project on the chemistry of 1,2,4-benzotriazine, we have reported a number of high-yielding synthetic routes to a variety of 1,2,4-benzotriazinyls.[9] The majority of these radicals are stable in terms of solid-state σ or π dimerization; only 1,3-diphenyl-7-(fur-2-yl)-1,4-dihydrobenzo[*e*][1,2,4]triazin-4-yl (**7FB**) (Chart 1) has a singlet ground state, arising from a $\pi-\pi$ interaction rather than a true bond, with a thermally excited triplet state.[7d] As part of our magnetostructural studies of 1,2,4-benzotriazinyls, herein we report 1-phenyl-3-trifluoromethyl-1,4-dihydrobenzo[*e*]-[1,2,4]triazin-4-yl (**3TB**), the first example of a hydrazyl radical that demonstrates a spin transition between a paramagnetic and a diamagnetic phase at $T_{sp} \approx 58(2)$ K.

Chart 1. Structures of 1,2,4-Benzotriazinyls

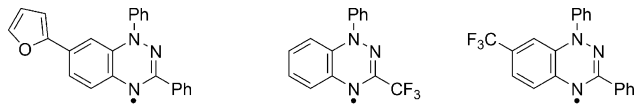

7FB **3TB** **7TB**

The recently reported synthesis of 3-trifluoromethylbenzotriazinyl **3TB** involved a multistep route that gave the radical in an overall yield of 37% [Scheme S1 in the Supporting Information (SI)].[9e] By applying Ma's copper-catalyzed C−N coupling protocol,[10] we were able to shorten the synthesis and improve the overall yield to 80% (Scheme S2). Radical **3TB** was purified by column chromatography (basic alumina, CH_2Cl_2) and was crystallized from a hot concentrated solution of *n*-pentane as dark-red needles. The intramolecular geometry, EPR spectral parameters, and cyclic voltammetry data for **3TB** are typical of other 1,2,4-benzotriazinyls (see the SI).

The magnetic properties of **3TB** were probed using a SQUID magnetometer. Variable-temperature magnetic susceptibility measurements were performed on a phase-pure polycrystalline sample of **3TB** (34.7 mg) from 5 to 300 K at two different applied

Received: June 25, 2014
Published: August 5, 2014

dx.doi.org/10.1021/ja5063746 | *J. Am. Chem. Soc.* 2014, 136, 11906−11909

fields (0.1 and 0.4 T). Data were collected in both warming and cooling modes with heating and cooling rates of 5 K min^{-1}. No significant differences between the sample susceptibilities obtained using different applied fields or temperature-collection modes were observed. Data were corrected for both sample diamagnetism (χ_{dia} = −146.5 × 10^{-3} emu mol^{-1}) and the diamagnetic contribution of the sample holder. As the sample was cooled from 300 to 60 K, the molar susceptibility (χ) increased following the Curie−Weiss law, with C = 0.377 emu K mol^{-1} and θ = −1.10 K (χ^{-1} vs T; Figure S5 in the SI), and reached a maximum at ca. 60 K (χ vs T; Figure S6). Within this temperature region, **3TB** behaved as a paramagnet with a stable χT value of ca. 0.374 emu K mol^{-1}, which is close to that expected for an S = $^1/_2$ paramagnet (Figure 1). Below 60 K the sample

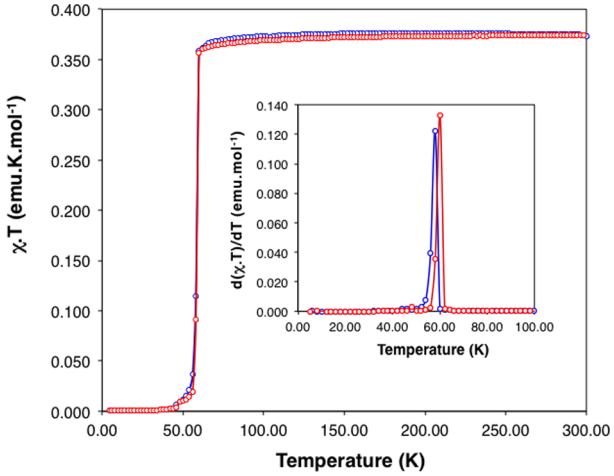

Figure 1. Temperature dependence of χT upon cooling (blue ○) and heating (red ○) for **3TB** between 5 and 300 K. Inset: graph of d(χT)/dT vs T showing full completion of the spin transition within 5(1) K and transition temperatures of 58 K (cooling) and 60 K (heating).

underwent a relatively sharp transition to a diamagnetic state with a small Curie tail at low temperatures attributable to 0.2% content of S = $^1/_2$ lattice defect sites. The low-temperature magnetic data (5−60 K) were fitted to the Bleaney−Bowers model[11] for the magnetic susceptibility of interacting pairs of S = $^1/_2$ spins ($\hat{H} = -2J_{12}\sum\hat{\mathbf{S}}_1\cdot\hat{\mathbf{S}}_2$), providing estimated values of $2J_{exp}$ = −166.8 cm^{-1}, g_{solid} = 2.0042, and ρ = 0.2% (Figure S7). This sharp discontinuity in the magnetic susceptibility occurred at T_{sp} ≈ 58(2) K and was not affected by the magnitude of the applied magnetic field. The transition was fully reversible in both the warming and cooling modes, showed no thermal hysteresis, and was completed within a narrow temperature range of 5(1) K (Figure 1 inset). The observed sudden change in the magnetic response of the sample denotes a first-order solid-state transition between two energetically similar structural phases.

To interpret the magnetic data and get a clear structural picture, we carried out a variable-temperature X-ray diffraction crystallographic study on a single crystal of **3TB**. Unit cell parameters were collected between 35 and 55 at 5 K intervals and between 55 and 60 at 1 K intervals in warming mode (Tables T2 and T3 in the SI). Full structural determinations were performed before and after the transition at 4 and 75 K (Table T4). No degradation in diffraction quality was observed despite cycling of the single crystal of **3TB** through the transition multiple times.

The triclinic space group $P\bar{1}$ was retained throughout the 4−300 K temperature region, indicating that the transition occurred without a major disruption of the intramolecular contacts and therefore without hysteresis. Unit cell parameters (Figure 2 and

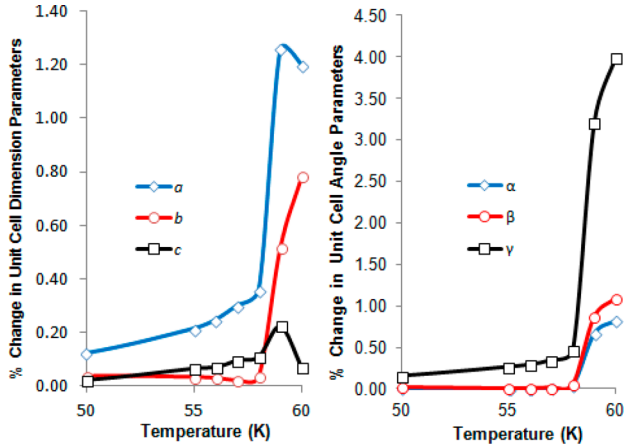

Figure 2. Percent changes in (left) the unit cell dimensions and (right) the unit cell angles with temperature for **3TB** from 50 to 60 K.

Tables T2 and T3) show that upon warming of **3TB** from 4 to 75 K, the nominally first-order transition is associated with a dramatic decrease in the angle γ by ca. 3.5° (4%), a decrease in the b axis by ca. 0.07 Å (0.8%), and an increase in the a axis by ca. 0.1 Å (1.3%) without a significant change in the cell volume (Table T4). The sharp structural transition occurred at ca. 59 K, confirming the spin transition of χ at T_{sp} ≈ 58(2) K. The observed changes in the three critical unit cell parameters are directly related to the solid-state packing arrangement.

Radicals of **3TB** π-stack to form 1D columns along the b axis (Figure 3). Within these columns, the radicals are related to each other through a center of inversion ($-x$, $-y$, $-z$) that places the N1-Ph groups on opposite sides, avoiding the buildup of steric congestion. The mean interplanar distance and the degree of slippage alternate along the stacking direction (Table 1). This gives rise to two distinct centrosymmetric pairs comprising radicals I and II and radicals II and III (Figure 3). At 75 K, the radicals of pair I−II are connected via a pair of weak symmetrical C−H···N interactions between N3 and an ortho hydrogen of N1-Ph [$d_{C9\cdots N3}$ = 3.572(2) Å, ∠C−H···N = 147.9(1)°; ($-x$, 2 − y, 1 − z)]. These interactions are absent in the 4 K structure, as a smaller longitudinal slippage angle between radicals I and II ($^{I-II}\phi_1$ = 13.8° at 4 K vs 21.2° at 75 K) increases the distance between the atoms.

The radicals of pair II−III are connected via short edge-to-face contacts. One set of contacts is common to both structures [$d_{C5\cdots C13}$ = 3.788(2) Å at 75 K and 3.763(2) Å at 4 K; ($-x$, 1 − y, 1 − z)], and the other appears only in the high-temperature phase [$d_{C4\cdots C13}$ = 3.600(2) Å; ($-x$, 1 − y, 1 − z)]. Radicals of neighboring stacks are connected in a head-to-tail orientation via an edge-to-face C−H···π contact between the fused benzene and N1-Ph [$d_{C5\cdots C13}$ = 3.745(3) Å at 75 K and 3.707(3) Å at 4 K] to form chains that run parallel to the a axis (Figure S8). Neighboring chains are connected in an antiparallel mode via a net of trans type-II C−F···F interactions of the CF_3 groups [$d_{F3\cdots F3}$ = 2.730(2) Å, θ_1 = θ_2 = 126.5(1)° and $d_{F1\cdots F1}$ = 2.690(1) Å, θ_1 = θ_2 = 163.9(1)° at 75 K; $d_{F3\cdots F3}$ = 2.677(1) Å, θ_1 = θ_2 = 135.0(1)° and $d_{F1\cdots F1}$ = 2.635(1) Å, θ_1 = θ_2 = 157.7(1)° at 4 K] to form ribbons in the ac plane (Figure S8). Similar C−F···F interactions link neighboring stacks in the crystal packing of **7TB**.[7a] While the two sets of C−F···F interactions and the short

dx.doi.org/10.1021/ja5063746 | J. Am. Chem. Soc. 2014, 136, 11906−11909

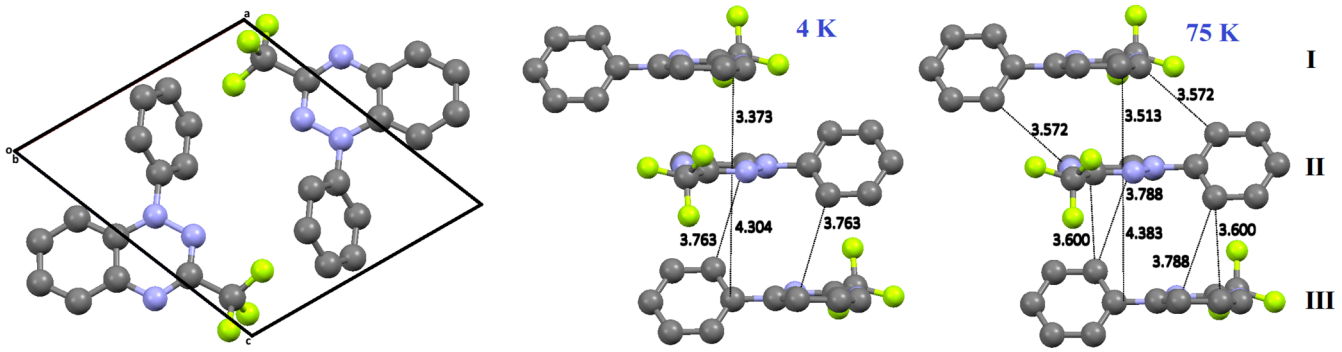

Figure 3. Unit cell of **3TB** viewed down the stacking direction (*b* axis) (left) and π-stacks of **3TB** at 4 K (middle) and 75 K (right) showing the shortest intermolecular contacts and the interplanar distances in pairs I–II and II–III. H atoms have been omitted for clarity.

Table 1. Slippage Angles and Interplanar Distances in Pairs I–II and II–III for Radical 3TB at 4 and 75 K

T/K	pair	$\phi_1{}^a$/deg	$\phi_2{}^a$/deg	d/Å
4	I–II	13.8	14.1	3.373
	II–III	11.5	35.7	4.304
75	I–II	21.2	7.8	3.513
	II–III	9.2	33.1	4.383

[a]See Figures S9 and S10 for definitions of the longitudinal (ϕ_1) and latitudinal (ϕ_2) slippage angles.

edge-to-face C···C contact appear in both the 4 and 75 K structures, a C–H···F interaction [$d_{C3\cdots F2}$ = 3.364(2) Å, ∠C–H···F = 134.4(1)°; (1 + *x*, *y*, *z*)] is present only in the low-temperature phase; upon warming from 4 to 75 K, the CF_3 group rotates from an N3–C1–C14–F3 torsion angle of 15° to 21°, breaking the C–H···F interactions (Figure S8).

The aforementioned intermolecular interactions are too weak to drive the interconversion between the two structural phases. Moreover, no significant differences were observed in the overall number of these interactions between the phases. Therefore, the lattice energy is mainly dominated by the SOMO–SOMO bonding overlap (see Figure 4). This is reflected in the transformation of the mean interplanar distance and the degree of slippage between radicals along the stacking direction (Table 1). A computational study by Robert and co-workers[12a] showed that the spin transition for the closely related verdazyl radicals[12b] was possible with a 0.4 Å increase in the intradimer equilibrium distance along with either a relative slippage (ca. 1.2 Å) or orientation (ca. 42°) of the verdazyl rings.

The phase transition of **3TB** occurred mainly via three significant structural changes taking place in the radical pair I–II: upon warming from 4 to 75 K, the interplanar distance (d_{I-II}) and longitudinal slippage angle ($^{I-II}\phi_1$) increased by ca. 0.14 Å and 7.4°, respectively, and the latitudinal slippage angle ($^{I-II}\phi_2$) decreased by ca. 6.3°. These changes are critical to the observed magnetic properties, as radicals of pair I–II interact mainly through the spin-bearing 1,2,4-amidrazonyl unit.

With a significantly smaller latitudinal slippage angle ($^{I-II}\phi_2$ < $^{II-III}\phi_2$) and shorter interplanar distance (d_{I-II} < d_{II-III}), radical pair I–II is anticipated to exhibit a stronger exchange coupling interaction than radical pair II–III ($|2J_{I-II}| > |2J_{II-III}|$). Therefore, in the absence of other dominating exchange interactions, $2J_{I-II}$ can be assigned to the exchange interaction determined by SQUID magnetometry ($2J_{exp}$ = −166.8 cm^{-1} from 5 to 60 K).

Direct estimates of the spin–spin exchange interactions within the radical pairs were provided by density functional theory (DFT) single-point calculations on the crystallographically determined geometries. We previously showed that for 1,2,4-benzotriazinyls the B3LYP functional combined with the unprojected equation[13] $J'_{12} = 2J_{12} = 2(E_{BS} - E_T)/S(S+1)$ where $S = S_1 + S_2$ and $S_1 = S_2 = 1/2$ (based on $\hat{H} = -J'_{12}\sum \hat{S}_1 \cdot \hat{S}_2$, where $J'_{12} = 2J_{12}$ to be equivalent to the spin Hamiltonian of the Bleaney–Bowers model) performed well in the computation of exchange interactions.[7e] The energies of the triplet (E_T) and broken-symmetry singlet (E_{BS}) states were determined at the UB3LYP/6-311++G(d,p) level (Table T5). The reasonable agreement between the calculated and experimental values [$2J^{DFT}_{I-II}$ = −184.8 cm^{-1} (4 K); $2J_{exp}$ = −166.8 cm^{-1} (5–60 K)] confirmed the dominating role of pair I–II (Table 2). At 4 K, pair

Table 2. UB3LYP/6-311++G(d,p)-Calculated Exchange Interactions[a] of Pair I–II ($2J^{DFT}_{I-II}$) and Pair II–III ($2J^{DFT}_{II-III}$) in their X-ray-Determined Geometries at 4 and 75 K

T/K	$2J^{DFT}_{I-II}$	$2J^{DFT}_{II-III}$	$2J_{exp}{}^a$
4	−184.8	−8.3	−166.8
75	4.1	7.0	

[a]Exchange interactions are given in cm^{-1}.

I–II adopts a more "superimposed" and shorter structure ($^{I-II}\phi_1$ = 13.8°, $^{I-II}\phi_2$ = 14.1°, d_{I-II} = 3.373 Å), giving rise to a multicentered two-electron interaction that quenches the paramagnetism (i.e., enhanced overlap in α-SOMO1 at 4 K vs 75 K; Figure 4). The exchange interactions in **3TB** are of the same magnitude as the ones previously reported for **7FB** ($2J_{DFT}$ = −244 cm^{-1} and $2J_{exp}$ = −172 cm^{-1} at 100 K), which has a singlet ground state dimer with a thermally accessible triplet state that is evident even at cryogenic temperatures ($|D|$ = 0.018 cm^{-1}, $|E|$ = 0.001 cm^{-1} at 5 K).[7d]

The rise of paramagnetism above 70 K for **7FB** was attributed to the population of the triplet state. A smooth second-order increase in the intradimer distance by ca. 0.076 Å leads to a relatively weakened exchange interaction and to a triplet exciton. However, even at 300 K the exchange interaction in **7FB** remained strongly antiferromagnetic ($2J_{300\ K}$ = −191 cm^{-1}), denoting a persistent spin pairing. Our results for **7FB** indicate that pair I–II in the low-temperature phase of **3TB** has a singlet ground state with a thermally accessible triplet state. With a rise in temperature the thermally excited triplet state becomes populated, leading to an increased net nonbonding interaction between the radicals. A large population of the triplet may cause the spin-paired dimer structure to collapse (via an increased interplanar distance) and consequently destabilize the lattice. While the gain in vibrational entropy most likely drives the

dx.doi.org/10.1021/ja5063746 | J. Am. Chem. Soc. 2014, 136, 11906–11909

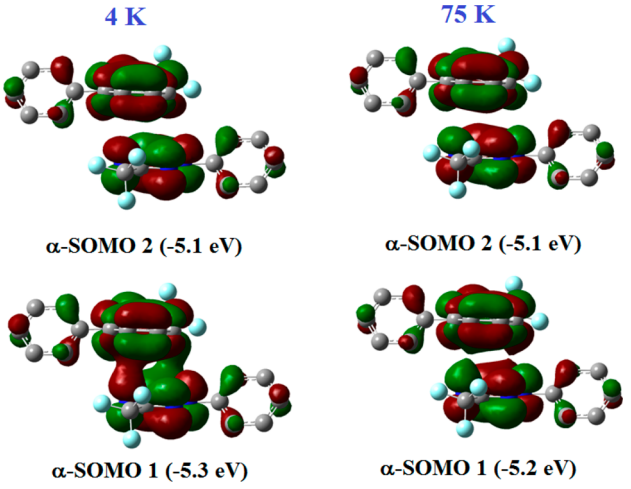

Figure 4. α-SOMO orbitals of pair I–II generated via UB3LYP/6-311++G(d,p) single-point calculations (triplet states) on the crystal structures determined at 4 and 75 K (visualized with an isovalue of 0.02).

transition from the low- to the high-temperature phase, the aforementioned intrastack mechanism of magnetism potentially assists the process. The calculated exchange interactions in the high-temperature phase have negligible magnitudes ($2J^{DFT}_{I-II}$ = 4 cm^{-1} and $2J^{DFT}_{II-III}$ = 7 cm^{-1} at 75 K; Table 2), indicating that the sudden rise in paramagnetism above 58 K stems from noninteracting $S = {}^1/_2$ spins within the weakly bound pairs I–II and II–III.

In summary, we have identified and investigated a rare spin transition of a low-molecular-weight radical composed exclusively of light atoms (C/N/F/H). 1-Phenyl-3-trifluoromethyl-1,4-dihydrobenzo[*e*][1,2,4]triazin-4-yl (**3TB**) is the first example of a hydrazyl radical that undergoes such a first-order transition and one of the few air- and moisture-stable radicals that demonstrate this behavior. The spin transition of **3TB** involves a low-temperature diamagnetic (S = 0) phase and a high-temperature paramagnetic ($S = {}^1/_2$) phase, occurs at ca. 58(2) K, is fully reversible, and compared with other examples is relatively sharp and completed within a narrow temperature range [5(1) K]. We are currently investigating the observed behavior under different external stimuli.

■ ASSOCIATED CONTENT

Ⓢ Supporting Information

Crystallographic (CIF), magnetic, EPR, CV, and DSC data and details of the improved synthetic route for **3TB**; instrumental analyses; computational methodology; and coordinates of atoms in pairs I–II and II–III used in computations. This material is available free of charge via the Internet at http://pubs.acs.org.

■ AUTHOR INFORMATION

Corresponding Author

koutenti@ucy.ac.cy

Notes

The authors declare no competing financial interest.

■ ACKNOWLEDGMENTS

This paper is dedicated to the memory of Prof. Michael Bendikov. The authors thank the University of Cyprus and the Cyprus Research Promotion Foundation for funding.

■ REFERENCES

(1) Ratera, I.; Veciana, J. *Chem. Soc. Rev.* **2012**, *41*, 303.
(2) (a) Lekin, K.; Phan, H.; Winter, S. M.; Wong, J. W. L.; Leitch, A. A.; Laniel, D.; Yong, W.; Secco, R. A.; Tse, J. S.; Desgreniers, S.; Dube, P. A.; Shatruk, M.; Oakley, R. T. *J. Am. Chem. Soc.* **2014**, *136*, 8050. (b) Wong, J. W. L.; Mailman, A.; Lekin, K.; Winter, S. M.; Yong, W.; Zhao, J.; Garimella, S. V.; Tse, J. S.; Secco, R. A.; Desgreniers, S.; Ohishi, Y.; Borondics, F.; Oakley, R. T. *J. Am. Chem. Soc.* **2014**, *136*, 1070. (c) Phan, H.; Lekin, K.; Winter, S. M.; Oakley, R. T.; Shatruk, M. *J. Am. Chem. Soc.* **2013**, *135*, 15674.
(3) Rawson, J. M.; Hayward, J. J. In *Spin Crossover Materials: Properties and Applications*; Halcrow, M. A., Ed.; Wiley: Chichester, U.K., 2013; Chapter 8.
(4) (a) Rawson, J. M.; Alberola, A.; Whalley, A. *J. Mater. Chem.* **2006**, *16*, 2560. (b) Barclay, T. M.; Cordes, A. W.; George, N. A.; Haddon, R. C.; Itkis, M. E.; Mashuta, M. S.; Oakley, R. T.; Patenaude, G. W.; Reed, R. W.; Richardson, J. F.; Zhang, H. *J. Am. Chem. Soc.* **1998**, *120*, 352. (c) Fujita, W.; Awaga, K. *Science* **1999**, *286*, 261. (d) McManus, G. D.; Rawson, J. M.; Feeder, N.; McInnes, E. J. L.; Novoa, J. J.; Burriel, R.; Palacio, F.; Oliete, P. *J. Mater. Chem.* **2001**, *11*, 1992. (e) Brusso, J. L.; Clements, O. P.; Haddon, R. C.; Itkis, M. E.; Leitch, A. A.; Oakley, R. T.; Reed, R. W.; Richardson, J. F. *J. Am. Chem. Soc.* **2004**, *126*, 14692. (f) Alberola, A.; Collis, R. J.; Humphrey, S. M.; Less, R. J.; Rawson, J. M. *Inorg. Chem.* **2006**, *45*, 1903. (g) Alberola, A.; Burley, J.; Collis, R. J.; Less, R. J.; Rawson, J. M. *J. Organomet. Chem.* **2007**, *692*, 2750. (h) Alberola, A.; Eisler, D. J.; Harvey, L.; Rawson, J. M. *CrystEngComm* **2011**, *13*, 1794.
(5) (a) Pal, S. K.; Bag, P.; Sarkar, A.; Chi, X.; Itkis, M. E.; Tham, F. S.; Donnadieu, B.; Haddon, R. C. *J. Am. Chem. Soc.* **2010**, *132*, 17258. (b) Mukai, K. *Bull. Chem. Soc. Jpn.* **1969**, *42*, 40. (c) Matsumoto, S.; Higashiyama, T.; Akutsu, H.; Nakatsuji, S. *Angew. Chem., Int. Ed.* **2011**, *50*, 10879.
(6) Hicks, R. G. *Org. Biomol. Chem.* **2007**, *5*, 1321.
(7) (a) Constantinides, C. P.; Koutentis, P. A.; Krassos, J.; Rawson, J. M.; Tasiopoulos, J. *J. Org. Chem.* **2011**, *76*, 2798. (b) Constantinides, C. P.; Koutentis, P. A.; Rawson, J. M. *Chem.—Eur. J.* **2012**, *18*, 7109. (c) Constantinides, C. P.; Koutentis, P. A.; Rawson, J. M. *Chem.—Eur. J.* **2012**, *18*, 15433. (d) Constantinides, C. P.; Carter, E.; Murphy, D. M.; Manoli, M.; Leitus, G. M.; Bendikov, M.; Rawson, J. M.; Koutentis, P. A. *Chem. Commun.* **2013**, *49*, 8662. (e) Constantinides, C. P.; Berezin, A. A.; Manoli, M.; Leitus, G. M.; Bendikov, M.; Rawson, J. M.; Koutentis, P. A. *New J. Chem.* **2014**, *38*, 949. (f) Constantinides, C. P.; Berezin, A. A.; Manoli, M.; Leitus, G. M.; Zissimou, G. A.; Bendikov, M.; Rawson, J. M.; Koutentis, P. A. *Chem.—Eur. J.* **2014**, *20*, 5388. (g) Yan, B.; Cramer, J.; McDonald, R.; Frank, N. L. *Chem. Commun.* **2011**, *47*, 3201. (h) Zheng, Y.; Miao, M.-s.; Kemei, M. C.; Seshadri, R.; Wudl, F. *Isr. J. Chem.* **2014**, *54*, 774. (i) Takahashi, Y.; Miura, Y.; Yoshioka, N. *Chem. Lett.* **2014**, *43*, 1236. (j) Bodzioch, A.; Zheng, M.; Kasynski, P.; Utecht, G. *J. Org. Chem.* **2014**, DOI: 10.1021/jo500898e.
(8) Blatter, H. M.; Lukaszewski, H. *Tetrahedron Lett.* **1968**, *9*, 2701.
(9) (a) Koutentis, P. A.; Lo Re, D. *Synthesis* **2010**, 2075. (b) Constantinides, C. P.; Koutentis, P. A.; Loizou, G. *Org. Biomol. Chem.* **2011**, *9*, 3122. (c) Berezin, A. A.; Constantinides, C. P.; Drouza, C.; Manoli, M.; Koutentis, P. A. *Org. Lett.* **2012**, *14*, 5586. (d) Berezin, A. A.; Constantinides, C. P.; Mirallai, S. I.; Manoli, M.; Cao, L. L.; Rawson, J. M.; Koutentis, P. A. *Org. Biomol. Chem.* **2013**, *11*, 6780. (e) Berezin, A. A.; Zissimou, G.; Constantinides, C. P.; Beldjoudi, Y.; Rawson, J. M.; Koutentis, P. A. *J. Org. Chem.* **2014**, *79*, 314.
(10) Xiong, X.; Jiang, Y.; Ma, D. *Org. Lett.* **2012**, *14*, 2552.
(11) Bleaney, B.; Bowers, K. D. *Proc. R. Soc. London, Ser. A* **1952**, *214*, 451.
(12) (a) Rota, J.-B.; Le Guennic, B.; Robert, V. *Inorg. Chem.* **2010**, *49*, 1230. (b) Koivitso, B. D.; Ichimura, A. S.; McDonald, R.; Lemaire, M. T.; Thompson, L. K.; Hicks, R. G. *J. Am. Chem. Soc.* **2006**, *128*, 690.
(13) (a) Novoa, J. J.; Deumal, M.; Jornet-Somoza, J. *Chem. Soc. Rev.* **2011**, *40*, 3182. (b) Noodleman, L. *J. Chem. Phys.* **1981**, *74*, 5737.